JPL PUBLICATION 80-55

High-Voltage Spark Carbon-Fiber Sticky-Tape Data Analyzer

Lien C. Yang
Glen G. Hull

June 15, 1980

National Aeronautics and
Space Administration

Jet Propulsion Laboratory
California Institute of Technology
Pasadena, California

JPL PUBLICATION 80-55

High-Voltage Spark Carbon-Fiber Sticky-Tape Data Analyzer

Lien C. Yang
Glen G. Hull

June 15, 1980

National Aeronautics and
Space Administration

Jet Propulsion Laboratory
California Institute of Technology
Pasadena, California

The research described in this publication was carried out by the Jet Propulsion Laboratory, California Institute of Technology, under NASA Contract No. NAS7-100.

FOREWORD

The work described in this report was performed by personnel of the Physico-Chemical System Group, Chemical and Biological Processes Section, Control and Energy Conversion Division. Dr. L. C. Yang was the Principal Investigator, Dr. K. Ramohalli was the Task Manager. The mathematical modeling was conducted by Mr. G. G. Hull. The hardware fabrication and calibration were performed by Messrs. H. Burris and T. Vo.

For reviewing the report and for their helpful comments, the authors thank Mr. W. L. Dowler, Group Supervisor, Dr. G. Varsi, Section Manager and Dr. V. L. Bell of Langley Research Center, the technical monitor of the project. Also thanks are due to Dr. C. L. Lawson for a helpful discussion on the mathematical modeling, to Mr. M. G. Farquhar for editorial assistance, and to Mrs. J. Howard and Mrs. M. Lipofsky for the typing of the report.

ABSTRACT

This report summarizes the development by JPL of an efficient method of detecting carbon fibers collected on a sticky-tape* monitor. The fibers were released from a simulated crash fire situation containing carbon fiber composite material. The project was part of NASA's "Carbon Fiber Risk Analysis" program, which was initiated to study the risk of such electrically conductive fibers being released in a fire or aircraft crash situation, and thereby posing a threat to electronic and electrical equipment.

In order to effectively determine the number and length of carbon fibers collected on the sticky-tape sample, a detection system other than visual examination was needed. The high voltage spark detection system reported here was developed by JPL for the NASA Langley Research Center between August 1979 and May 1980. It uses the ability of a carbon fiber to initiate spark discharge across a high voltage biased grid to achieve accurate, rapid, and automatic counting of fibers on the tape. The design of the system was optimized, and prototype hardware was proven satisfactory in laboratory tests.

* This is the common name used for instrumentation applications of the several plastic based materials that are coated with an adhesive material which is thick and fluid enough to retain particles or impressions. Commercially they are marketed as pressure sensitive tapes. The material used for this work has a commerical trade-name "Clear Adheer".

TABLE OF CONTENTS

LIST OF FIGURES

LIST OF TABLES

I. INTRODUCTION

Historically, sticky tape* has been the technique most widely used for monitoring carbon fiber exposure. (References 1,2,3). It is inexpensive, easy to use, and the test results can be stored and retrieved for later measurements. All these features are very suitable for carbon fiber field tests in which one aim is to monitor the fiber fragments exposure in several hundred locations.

The technique has its disadvantages and limitations, however. Notable handicaps are the following:

1) Data Reduction. Due to the small diameter of the fiber, typically 6 to 8μ, visual counting of the fiber fragments invariably requires the use of a magnifying system, usually a microscope. This counting operation always has been tedious and slow.

2) Lack of Dynamic Information. The tape is an integration device. It accumulates the total number of fibers intercepted by the tape during a period of time. Information such as the fiber flux as a function of time cannot be determined directly. Remedies for this deficiency, such as incremental exposure, are tedious, if not impractical.

3) Calibration and Data Interpretation. Just as in any other fiber detection instrument, the detection or sticking efficiency depends upon a variety of physical conditions, such as the geometry of the tape, the air flow rate, the angle of incidence, etc. The efficiency factor is usually less than 100%. Some preliminary studies at JPL indicated that the efficency is only about 5 to 10% for cylindrical tape (sticky cylinder) (Reference 4). Such low capture efficiencies create uncertainties in the determination of the total fiber count.

4) Saturation Effect. There are indications that the ability of the tape to collect the fiber fragments deteriorates with accumulated fiber fragments and soot. The latter usually occurs during a carbon fiber composite burning test. (Reference 3).

Despite these difficulties, the advantages of using the tape are still overwhelming, and it is anticipated that it will continue to be used for the study of carbon fibers.

The present work deals mainly with problem 1), the readout of the tape. The new technique uses the ability of the fiber to initiate a spark across a set of alternately biased high voltage electrodes to electronically count the number of fiber fragments collected on the tape. Automatic high rate counting can be achieved. The technique is a spin-off of the previous development of a live high-voltage spark carbon-fiber detection system (Reference 4). In that effort, the fiber fragments suspended in the air were sampled by passing them through parallel strip grids of different spacing. Upon alignment by the high voltage electrical field of the grid, the fibers bridged the electrodes of the grid and caused shorting. The energy stored in a capacitor of the bias circuit was then released to form a spark in the air between the electrodes. The peak current of the pulse discharge was used to trigger a counter-integrator circuit for counting the number of fibers passing through the grid.

---

* See page iv

It was found that the spark, which contains high energy and is of very short duration, is capable of partially damaging or consuming the fiber fragments. It also creates a mechanical disturbance which ejects the fibers from the grid. Both characteristics were helpful in establishing a single discharge pulse for each fiber segment.

In that development effort, in order to characterize the peak current as a function of the operating parameters such as the grid bias voltage and fiber length, a stationary test was performed. (Reference 4, Section IV). In that test, a fiber segment was placed across a grid. The electrodes were initially isolated from the high voltage circuit by a spark gap (krytron) so that it was not biased by the high voltage. Upon receiving a trigger command, the spark gap was actuated, the grid became biased, and a high voltage spark was initiated by the fiber. This technique allowed a controlled placement of the fiber with respect to the electrodes. It also made possible the synchronizing of the discharge and the camera shutter, so that photographs of the spark phenomenon could be recorded under a microscope.

The spark was always found to proceed across a single fiber segment, even though there were many fibers laid across the grid. There were considerable variations in the contact resistances between each fiber and the electrodes of the grid. The spark, which is a transient avalanche discharge phenomenon, followed the path of lowest resistance. After the spark, the fiber was partially damaged and consumed, thereby reducing its ability to initiate a spark. The next spark was usually initiated by another fiber segment across a pair of adjacent electrodes of the grid. Thus, under a repeated actuation (triggering) of the stationary test circuit, the spark occurred at different fiber bridges across the grid. The action was terminated when there were no fiber segments capable of initiating the spark under the fixed test conditions.

The total number of discharges is thus directly proportional to the number of fiber segments bridging the grid. By monitoring this quantity, it is possible to determine the number of carbon fiber segments collected on a sticky tape. Furthermore, the trigger mechanism of the apparatus can be designed to repeat at a high rate, so that fast spark initiation can be achieved. Automated fast counting of carbon fibers on a sticky tape can be accomplished by this procedure.

The sticky tape read-out technique was first suggested to Dr. V. L. Bell of Langley Research Center on February, 1979. Instrumentation development was initiated as part of the carbon fiber detection system effort. Hardware was fabricated in the summer of 1979 and calibration of the device was completed in the spring of 1980.

II. DESIGN OF THE SYSTEM

A. Design Considerations

The general characteristics of the carbon-fiber-initiated high-voltage spark phenomenon, such as physical mechanisms, electrical characteristics, and destruction of the fiber, are the same as described in Reference 4. The presence of the sticky tape affects the following areas:

1) Count efficiency. The fiber segments are physically held down by the tape and, unlike the high voltage spark real-time carbon fiber detection system, are not free to align with the electrical field between the grid electrodes. Thus, the fiber segments on the tape, which orient randomly, may not align in a favorable position to generate a spark. The number of intersections between the grid electrodes and a long fiber obviously depends upon the orientation of the fiber relative to the grid electrodes. Thus the count efficiency of the system has to be determined and interpreted statistically.

2) Spark structure. In the presence of the tape the spark will be asymmetric, i.e., instead of forming isotropically in the air surrounding the fiber, the spark will pass through the air above the fiber. The shock generated by the spark thus tends to press the fiber onto the tape instead of ejecting it from the electrode. Post-spark examination has shown that partially-damaged fiber fragments remained on the tape and that no fibers were released by the spark process.

3) Thermal destruction of the fiber by the spark. Both the change of spark pattern as described above, and the additional heat loss due to the heat sink effect of the tape, may reduce the efficiency of the destruction of the fiber by the spark.

The effects of 2) and 3) described above will enhance the chances for survival of the fiber in a spark, and therefore multiple sparks will be generated by a single fiber bridge across a pair of adjacent electrodes. This multiple counting effect complicates the interpretation of the test result.

B. Choice of The Grid

The No. 1 grid developed for the high-voltage spark real-time carbon-fiber detection system (Reference 4) was chosen as the working grid for the sticky tape analyzer. It has a grid spacing (i.e., air gap) of 1.19 mm (0.047 in.) between pairs of electrodes. The electrodes were made from 0.508 mm (0.020 in.) thick copper strips. They were 0.95 cm wide and about 9.65 cm in length. One end of the strip had a slotted tab to permit the solder connection. About 35 electrodes were used to form a grid aperture of 6.0 cm x 9.65 cm in a Teflon frame. This area is sufficient to accommodate sticky-cylinder-type tape samples. Under a bias voltage of 510 V, this grid can generate a spark when the projected length of a fiber segment (along the direction of the closest distance between a pair of adjacent electrodes) exceeds 1 mm. This sensitivity is appropriate since the result of NASA's Carbon Fiber Risk Analysis Program has indicated that the lengths of carbon fiber fragments released from a fire of carbon fiber composite lie mainly in the region of 1 to 5 mm.

In the beginning of the development, the plan was to use a set of five grids with different spacings, similar to that in Reference 4, to diagnose fiber length. This approach was abandoned because of the difficulties in preparing long fiber tape samples for calibrating grids with large grid spacing. A theoretical analysis (Section VI) has indicated that most relevant information can be retrieved from the tape by using the No. 1 grid described above. This choice of grid also has improved the operating safety of the system because only 510 V is required to operate the No. 1 grid. The required voltages for grids with larger grid spacing are considerably higher, ranging from 680 to 1200 V for grids No. 2 to 5.

C. Counting Rate

Similarly to the high-voltage (H.V.) spark real-time carbon-fiber detection system, the rate capability is primarily limited by the current capability of the high-voltage power supply.

$$\text{Counting rate} = I/CV$$

$$= 5.32 \times 10^3 \, I/V$$

where

I = H.V. power supply current in mA

V = H.V. power supply voltage in volts

C = capacitance of the discharge capacitor in farads

= 0.188 μF

For safety of operation, a low current H.V. power supply should be used for the test. A dry battery pack containing a single Eveready No. 497 battery (510 V) is suitable for bias of the discharge circuit. The battery has a short term maximum current capability of about 10 mA. Therefore, a maximum counting rate of 100 counts per second (Hz) can be reached by using this battery. This rate is suitable for reducing fiber number d on a typical tape sample, such as a sticky cylinder. The tape usually collects several hundred fiber fragments in an area of 40 x 40 mm. Thus the tape can be read in less than a minute with a counting rate of 10 counts per second (Hz).

D. Electronic Package

The electronic circuit consists of two parts: the high-voltage pulser circuit, which is the same one used in the stationary test of a carbon fiber described in Reference 4, and the trigger circuit which controls the actuation of high-voltage pulser. (Figures 1 and 2).

1. High-Voltage Pulser. The energy storage capacitor bank consists of four 0.047 μF high-voltage capacitors, C_1, C_2, C_3, and C_4 (CDC PKM 16S47, 1600 VDC rating), connected in parallel. It provides a discharge energy for about 24 mJ at a voltage of 510 V. The miniature spark gap EG&G KN-22 was used to isolate the grid from the pulse discharge circuit as described previously. It was chosen over a conventional SCR because of its high current rating. It has the following ratings:

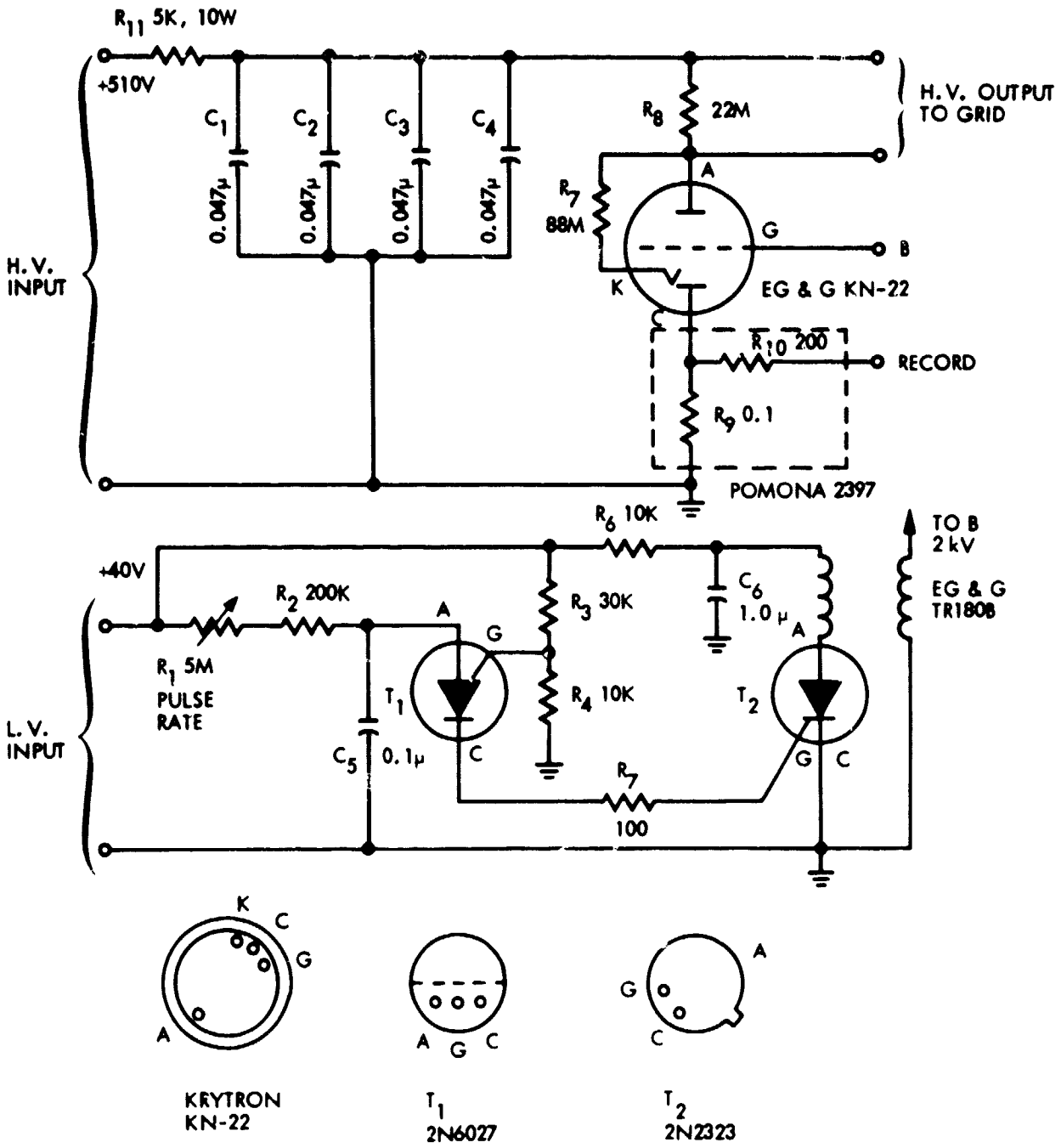

Fig. 1. Schematic Circuit Diagram for the H.V. Discharge Electronic Package

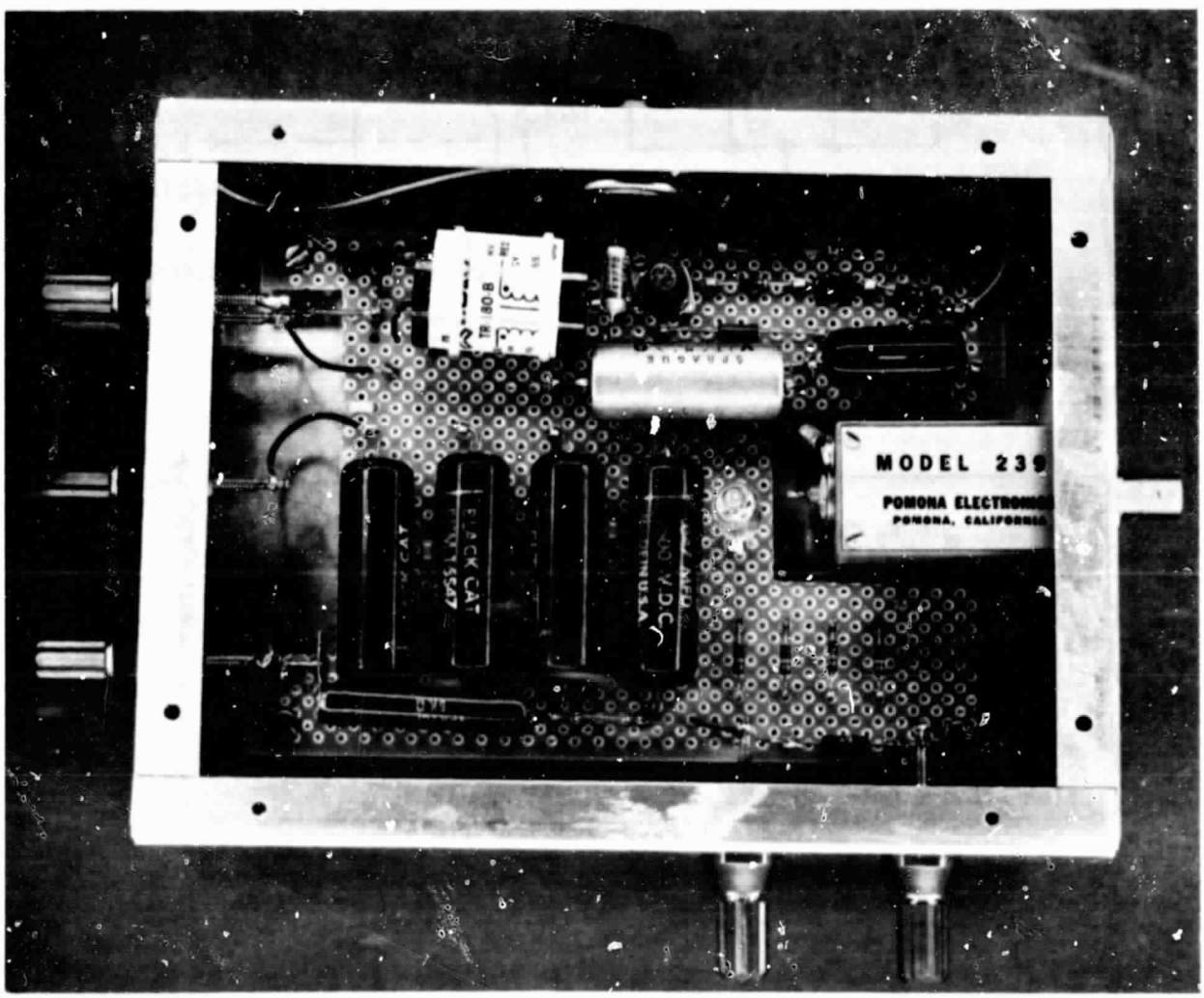

Fig. 2. Layout of Components of the H.V. Discharge Electronic Package.

Maximum voltage : 5000 V

Minimum voltage : 400 V

Maximum peak current : 100 A

Minimum trigger voltage : 750 V

Size : 1.0 cm diameter
2.2 cm length

The life expectancy of the spark gap depends upon discharge conditions. For short pulse durations of 0.04 μs and a pulse rate of 50 Hz at 80 A peak current, it is rated for a life of 2×10^7 operations. For longer and/or faster pulse rates the life may be reduced. In our tape reader design, the peak discharge current is about 100 A and the pulse duration is about 1 μs. Therefore, a nominal 5 to 15 Hz pulse rate is recommended for long duration counting. A fast counting rate, up to the maximum rate of 100 Hz, can be used for short duration tests of the order of 10 seconds or less. The limiting factor is the heat dissipation, which is related to the small size of the unit. These faster rates are preferred for tape reading because the number of carbon fibers collected on a sticky cylinder is usually less than 1000. To achieve a higher discharge rate a large size spark gap, such as the GP series ceramic-metal triggered spark gaps manufactured by EG&G, Inc., would have to be used for the design. Under the designed discharge condition, the tape reader has been used for about 100,000 discharges, with no sign of degradation in performance.

The 22 mega-ohm resistor, R_8, is necessary (see Figure 1) to establish an initial voltage across the grid (fiber)--a condition necessary for overcoming the contact resistances between the grid electrodes and the fiber. The 88 mega-ohm resistor, R_7, provides a low keep-alive current (∿5 μA)--a condition which enhances the fast actuation of the krytron.

The 0.1-Ω resistor, R_9, is a current shunt for monitoring the discharge current. The output signal is available at the RECORD for conveyance by a 50-Ω impedance coaxial cable to a digital counter via a 50-Ω terminal resistor. The latter and the 200-Ω resistor, R_{10}, form a potential divider for reducing the current signal to an amplitude of about -5 V. This part of the circuit is contained in a Pomona Box 2397, for better noise reduction.

2. Trigger Circuit. The high-voltage trigger pulse (∿2 KV) for actuation of the krytron is provided by the output of the trigger transformer, an EG&G TR 180B. The discharge of the capacitor, C_6, through the primary coil of the transformer is controlled by an SCR (2N2323), T_2. This, in turn, is controlled by the pulse generated by a circuit formed by a programmable unijunction transistor (2N6027), T_1. The discharge of the capacitor, C_5, to trigger the SCR, T_2, will occur every time the voltage across the capacitor reaches 10 V. This rate of occurrence is determined by the time constant $(R_1 + R_2)C_5$. By adjusting the potentiometer, R_1, PULSE RATE, a pulse discharge rate of 5 to 100 Hz can be achieved. As described previously this rate allows the full charge of capacitors C_1 to C_4 by the H.V. battery.

E. Current Pulse Shape

Figure 3 shows a typical oscillogram of the discharge current pulse. As was shown in Reference 4, the phenomenon is basically an RLC discharge, where $C = C_1 + C_2 + C_3 + C_4 = 0.188$ μF. R is the arc resistance of the spark and L is the circuit inductance. The wave form is oscillatory because the condition $R^2 - 4L/C < 0$ is satisfied. R will change depending upon the orientation of the fiber with respect to the electrodes of the grid. R reaches its smallest value (high peak current) if the fiber is perpendicular to the electrodes. As the fiber orientation becomes oblique to the electrodes, R will increase and the peak current will decrease. By choosing a larger value for L, the variation of peak current can be minimized so that a digital counter of fixed trigger sensitivity can record all the pulses. This condition was satisfied by using long lead wires, 30 to 45 cm long, to connect the grid to the discharge electronic package.

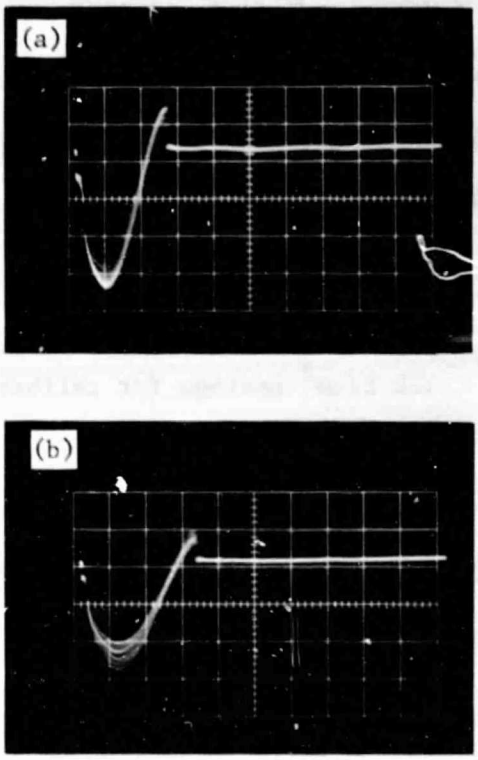

Fig. 3. Discharge Current Pulse Characteristics, 1.0 V/Div., 0.5 μs/Div., a) 5 cm Long Lead Wires, b) 30 cm Long Lead Wires

III. GENERAL DESCRIPTIONS AND SPECIFICATIONS

The JPL high-voltage (H.V.) spark carbon-fiber sticky tape analyzer was developed to detect the number of carbon-fiber fragments with lengths in excess of 1 mm. It simply consists of three subassemblies.

1) The Grid. The grid is made of a number of equally-spaced, parallel copper blade electrodes secured in a frame made from an electrically insulated material (Teflon). The electrodes are periodically biased by high-voltage discharge circuitry. Hence, when a sticky tape containing carbon fiber is in contact with it, an H.V. spark will be initiated.

2) High-Voltage Discharge Circuit Electronics. This subassembly provides a high-voltage bias to the grid when the discharge capacitor is fully charged. The discharge current pulse signal is available at the output of the package to trigger a digital counter.

3) H.V. Battery. The battery energizes the discharge circuit.

The following is a list of the general specifications for the system:

1) Detectable fiber lengths: 1.0 mm to 6.0 cm.

2) Counting Rate: 5 to 100 Hz

3) Tape Size: 6.0 x 9.5 cm maximum

4) Fiber density: 120 f/cm^2 maximum for calibarated application

5) Sensivity: $N = C/k\ell_o$

$L = C/k\ (1 + 1/\ell_o)$

where

N = total number of fiber fragments on tape

L = total length of fiber fragments on tape

C = total counts registered by the digital counter

k = calibration factor = 0.898 mm^{-1}

ℓ_o = $\bar{\ell}$ - 1 in millimeters = 2.2 mm

$\bar{\ell}$ = average fiber length in millimeters

These formulae are derived under the assumption that a priori knowledge of the fiber length distribution is known. The distribution is given by

$$n(\ell) = e^{-(\ell-1)/\ell_o}$$

where ℓ = length of a fiber fragment
$n(\ell)$ = number of fiber fragments with length ℓ

Note that

$$\int_1^\infty n(\ell)\, d\ell = 1,\ 1\ \text{mm} < \ell < \infty$$

The complete derivation is included in Section V.

6) Accuracy : approximately ±10%

7) Grid:

Active area = 6.0 m x 9.5 cm

Electrode spacing (air gap) = 1.19 mm
Electrode thickness = 0.508 mm
Electrode material: copper
Frame material: DuPont Teflon
Frame dimensions: 11.4 cm long
8.6 cm wide
1.4 cm high
Weight = 260 g
Number of electrodes = 35
Maximum applicable voltage = 2000 V
Design voltage = 510 V
Polarities: Interchangeable

8) H.V. discharge electronics:

DC input = 40 V nominal
30 V operable
Maximum H.V. input = 1600 V
Designed H.V. input = 510 V
Pulse rate: adjustable, 5 to 100 Hz
Signal output = -5 V nominal when 50 Ω terminal is used
Length of lead wires to the grid = 30 to 45 cm
Case: 20.3 x 15.2 x 5.1 cm aluminum box with top lid made of Lucite
Weight: 690 g

9) Battery Pack:

Consists of a single Eveready No. 497 battery contained in an aluminum box.

Output = 510 V
5 mA nominal
10 mA transient
Package size: 5.1 x 10.2 x 20.3 cm
Package weight: 990 g

As mentioned previously, the use of this battery pack is recommended over other H.V. power supplies due to its operating safety.

10) Input, output, and control elements of the system.

H.V. Discharge Electronic (Figures 4a and 4b)

H.V. INPUT : banana posts
red: + black: -
connect directly to H.V. battery pack

H.V. OUTPUT : banana posts
red: + red: -
connect to the electrodes of the grid; interchangeable

L.V. INPUT : banana post
red: + black: -
for input of 40 VDC

RECORD : receptacle BNC terminal for connecting the discharge current pulse signal to the digital counter (with an input load of 50 Ω).

PULSE RATE : one-turn dial control

BATTERY PACK : Two H.V. outputs, banana posts
Red: + black: -
Voltage: 180 V (not used)
510 V (used for the system)
Both outputs have safety on-off control (key).

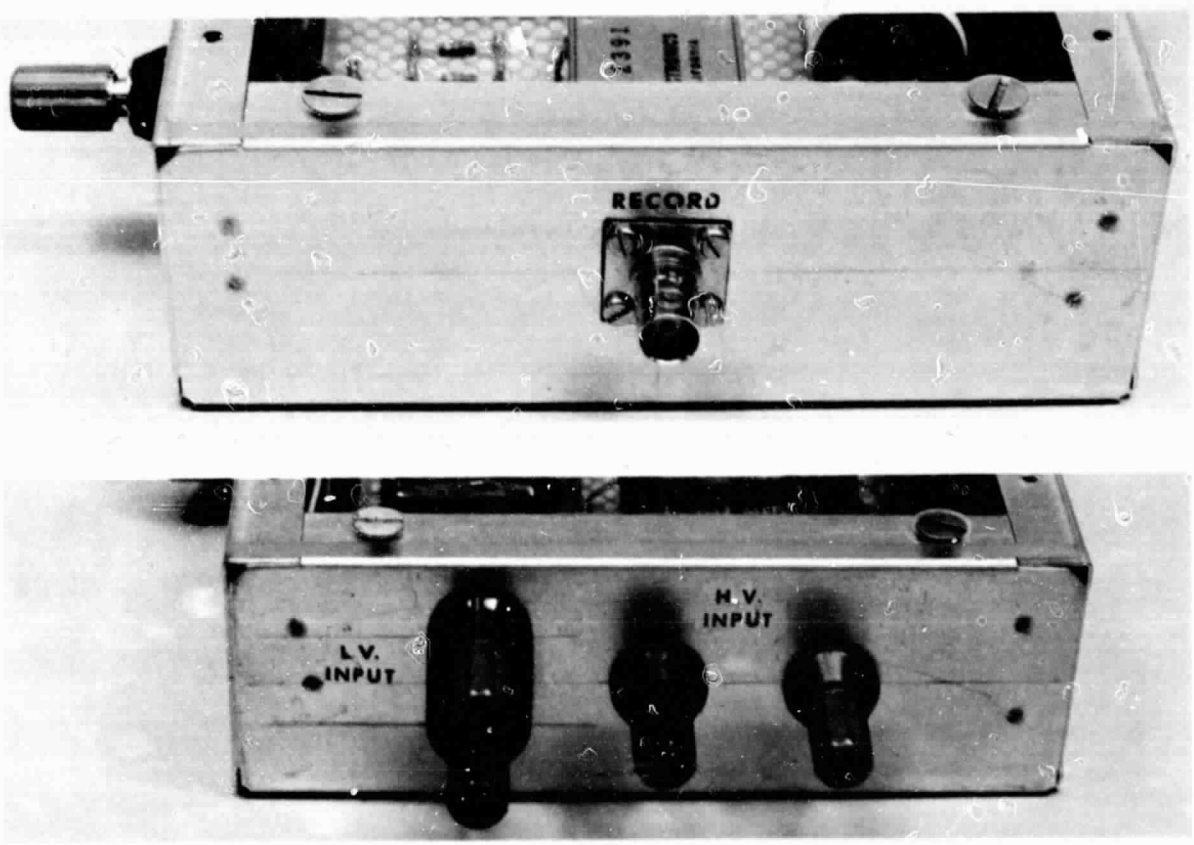

Fig. 4a. Controls and Interface Terminals of the H. V. Discharge Electronics Package

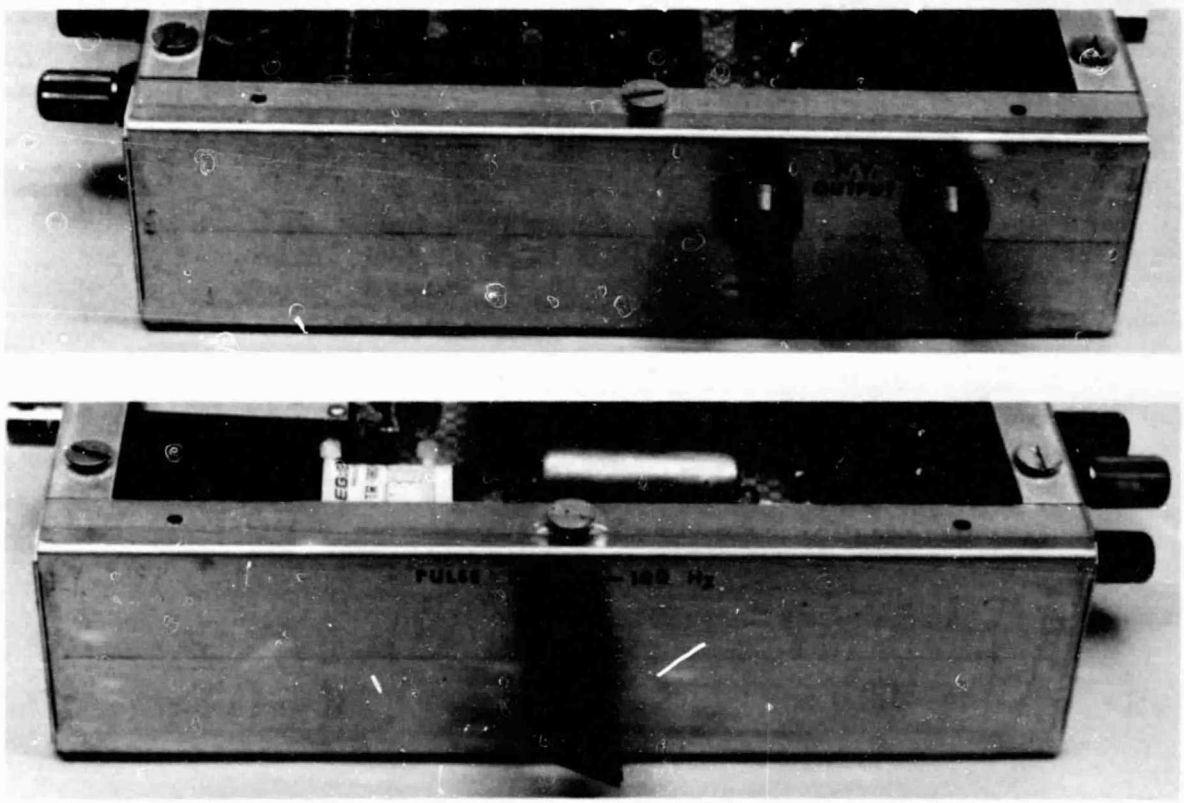

Fig. 4b. Controls and Interface Terminals of the H.V. Discharge Electronics Package (Continued)

IV. OPERATING PROCEDURES

The following operating procedures should be observed (refer to Figure 5):

1) Beware of exposed high voltage in the system; handle with the same precautions used for any high voltage device.

2) Check grid insulation by connecting a Simpson or other multimeter across the electrode bus wires of the grid. On the x10,000 Ω scale, the reading should indicate an open circuit.

3) Lay the grid on an insulated table or platform with the exposed electrode facing upward.

4) With all power off, connect the grid to the H.V. OUTPUT terminal on the H.V. discharge electronics package with two insulated test leads, 30 to 45 cm long. The connection to the grid should be made by alligator clips securely attached to the bus wires. (Later versions of the grid are provided with banana posts for snap-on connections of the wires).

5) Connect the 510 V OUPUT on the battery pack to the H.V. INPUT terminal on the H.V. discharge electronics package with two insulated test leads.

6) Connect a 40 VDC power supply to the L.V. INPUT terminal on the H.V. discharge electronics package.

7) Connect the RECORD on the discharge electronics package to the input of a digital counter using a 50Ω coaxial cable with a 50Ω terminal load. A counter with an input trigger level adjustment and a low pass filter, such as the FLUKE Model 1900, is recommended. The filter should have a cut-off frequency of about 1 MHz. Set the counter in the Integration or Total Mode.

8) Place the sticky tape on the grid, lightly pressing the tape so that it sticks to the electrodes.

9) Set the PULSE RATE control to the lowest value (∿5 Hz) by turning the dial knob fully counter-clockwise.

10) Turn on the 40 VDC power supply. Observe the faint, pulsing arc in the krytron as seen through the Lucite top plate of the discharge electronics package.

11) Turn on the 510 V H.V. battery pack by actuating the key on the pack. Spark discharges will occur on the tape, initiated by the fiber fragments on the tape bridging the electrodes of the grid.

12) The sparks should have a bright white-blue color and occur one at a time. The sparks should move around on the tape as fiber segments bridging adjacent pairs of electrodes are being destroyed. The crisp sound of the sparks should be heard.

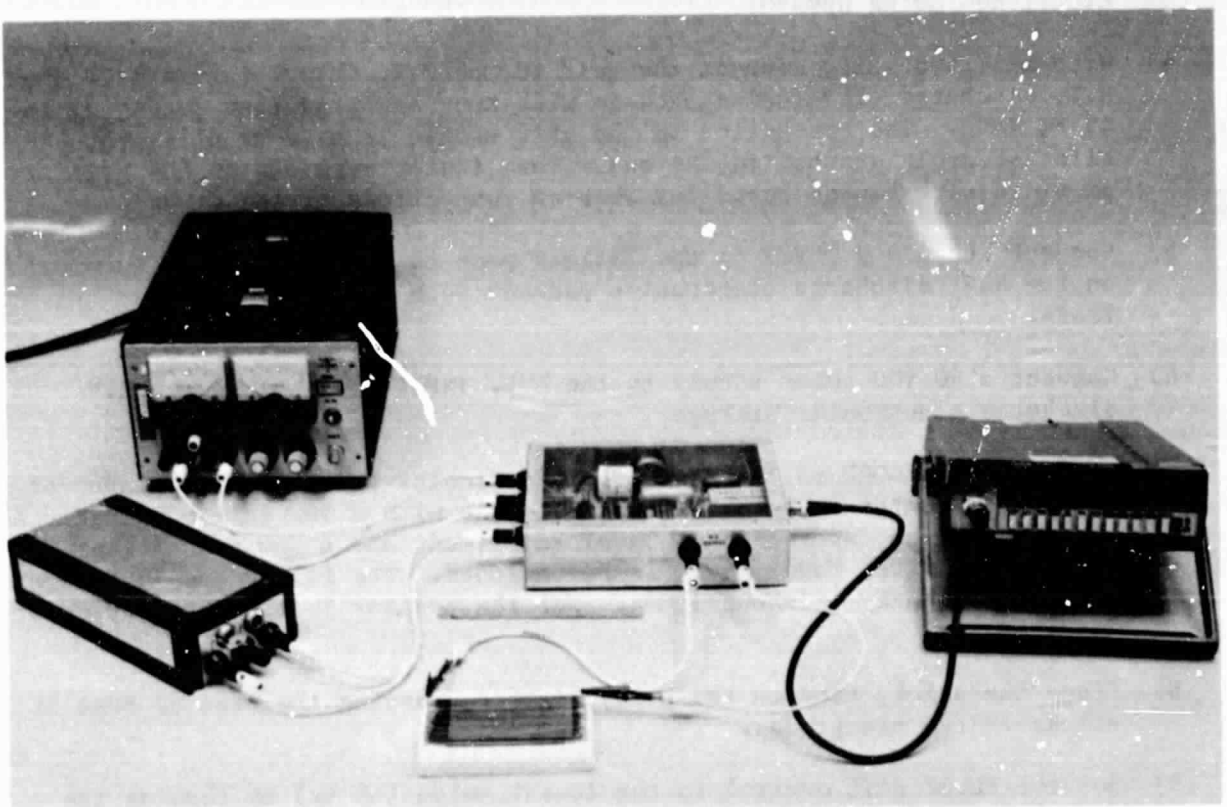

Figure 5. Test Setup of the System

13) Observe the digital counter registering the number of sparks. Make sure each spark causes one and only one count.

14) To increase the counting rate, the PULSE RATE can be increased by turning the control knob clockwise. If the counting procedure is not completed in less than 10 seconds, do not use the maximum rates.

15) The counting procedure will automatically terminate when there are no fiber segments on the tape capable of producing a spark.

16) Simultaneous arcing across many fiber segments occurs if the number of fibers on the tape is excessive. These arcings have a yellowish color and produce no crisp sound although the digital counter may continue to record. If so, however, this is a false counting, because the current passing through the fibers is low and the fibers are not being destroyed. If this occurs, immediately turn off the H.V. battery pack by turning the safety key, reset the digital counter, and perform the following procedures.

17) Discharge the residual charge across the grid by shorting the grid. An easy and safe way is to insert the lead point of a wood stick type pencil in a gap between any pair of adjacent electrodes. A single spark will be initiated to discharge the system.

18) Peel the tape from the grid. Reattach it in the manner shown in Figure 6a, i.e., with only part of the tape in contact with the grid electrodes. Turn on the H.V. battery pack; correct fiber counting should commence.

19) When the spark count stops, put more tape in contact with the grid to continue the process. This should be done gradually by using any insulated stick, such as the pen eraser shown in Figure 6b.

20) When the counting is completed, record the number showing on the digital counter. Turn off the H.V. battery pack. Discharge the grid and remove the tape from the grid.

21) Infrequently, the electrodes of the grid need cleaning as the glue from the tape may accumulate on them. This can be done by rubbing the electrode plane with an ink eraser containing an abrasive grit and by wiping the electrodes with an acetone-soaked cloth.

22) In case of emergency or abnormal functioning of the system, the first step is to turn off the H.V. battery. The following describes several possible malfunctions of the system.

23) The persistent occurrence of the spark at one fixed location on the tape is normal and is caused by a thick fiber fragment, a fiber rod or fiber stick containing a large number of single fibers. The fragment may create a large number of sparks, and eventually it will burn out.

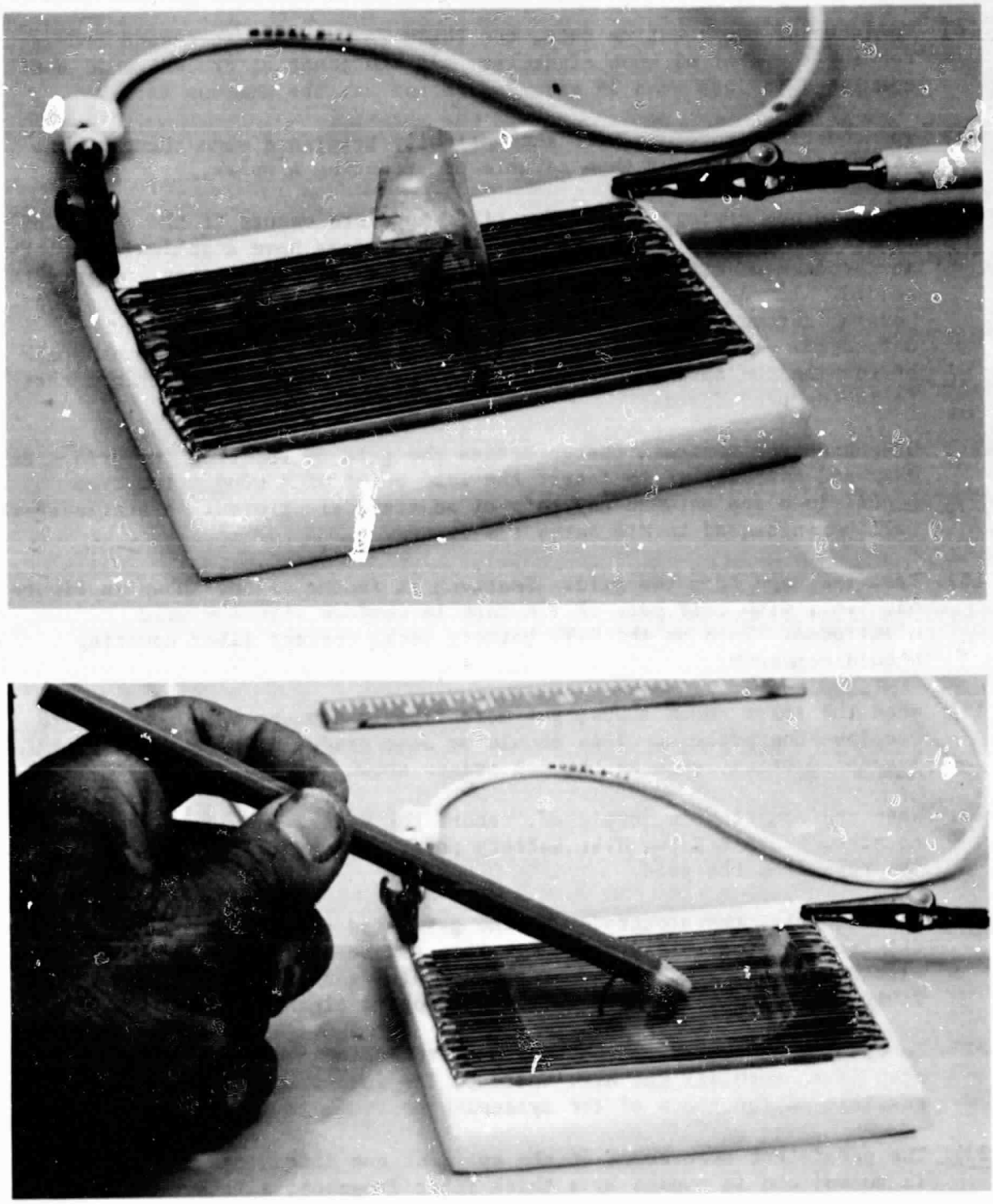

Fig. 6. Method of Applying the Tape Sample on the Grid

24) Two failure modes of the krytron are possible. First, it may fail to turn off after discharge, thereby remaining in a conducting state and draining the battery. This condition is indicated by the bright illumination of the krytron tube accompanied by no sparking. This sometimes occurs when the pulse rate is high and there are thick fiber fragments on the tape. The rate should be reduced in order to eliminate the problem. Second, the krytron may overheat and crack, causing air to leak into the tube and the krytron to cease conducting. In this case, the spark will not occur and the tube must be replaced.

25) The output voltage of the H.V. battery pack should be checked periodically. When its value falls below 490 V, replacement is recommended. The procedure is simple, but caution is required because of the high voltage. Gloves should be worn when soldering wires inside the battery pack.

V. EXPERIMENTAL CALIBRATION

A. Calibration Requirements

The mathematical analysis in Appendix A shows the fundamental principle of operation of the H.V. spark carbon-fiber tape analyzer. However, in order to make the system practical, the following additional information and verification is needed and can only be determined by experimental means.

1. The Multiple-Count Effect. This phenomenon has been discussed in Section II. More than one mechanism is involved in the damaging of fiber segments lying across a pair of adjacent electrodes, preventing them from further initiating H.V. sparks. These mechanisms are not fully understood. Thus, the average number of counts generated by a single fiber segment can only be determined experimentally.

2. The Discharge Criterion. The H.V. imposed on the grid can overcome the contact resistance between the fiber and the electrodes when they are in contact. It also can initiate sparks when gaps exist between the ends of the fiber fragment and the electrodes. A gap equal to 16% of the distance between electrodes was found capable of producing sparks during the calibration of the H.V. spark real-time carbon-fiber detection system (Reference 4). In that case the fiber fragments, being suspended in the air, are free to align perpendicularly to the electrodes. In a tape, the fiber will orient in a completely random manner with respect to the electrodes, and the electrical breakdown condition may be different. The 16% figure was used in the mathematical analysis.

3. The Effect of a Fiber Rod. When a large number of fibers form a bundle, they will initiate a single spark. The spark, being very extensive in dimension, will be the same as that initiated by a single fiber. However, the interaction between the spark and the fibers in the bundle is more complicated. Accordingly, destruction of the fibers in the bundle may proceed differently than in the case of a single fiber, resulting in multiple counts.

4. The Effect of Fiber Linkage. When the number of fiber fragments in a tape is large, linkage between fibers is inevitable and may increase the probability of spark generation. This situation was too complicated to be included in the mathematical analysis in Appendix A. The consequences of linkage must be revealed by experimental calibration.

B. Baseline Calibration

The aim of this part of the test activity was to determine the number of spark counts per fiber bridge across a pair of adjacent electrodes. The sticky tape used for the test was 0.05 mm thick "Clear Adheer" laminated mylar sheet manufactured by C-Line Products, Inc. Large sheets were cut into small pieces for testing on the grid. Long lengths of a single fiber, or a fiber bundle containing several single fibers, were implanted on each single tape. The samples were then placed on the grid with the fiber oriented at a selected angle with respect to the grid electrodes. The number of fiber bridges were counted under a microscope. The grid electronics were activated and the spark counts recorded. Typical results are shown in Table 1.

Table 1. Spark Counts per Fiber Bridge

Angle of Fiber With Electrodes	No. of Fibers, f	Fiber Bridges, Per Fiber, n	Total Counts C	C/nf
90°	1	27	77	2.85
	1	26	59	2.27
	2	24.5	114	2.19
	3	26	167	2.14
	1	26	58	2.23
	1	27	67	2.48
	1	11	32	2.91
	1	30	81	2.70
	1	27	65	2.41
45°	1	13	35	2.69
	1	11	26	2.36
			Average	2.475

Tests of the fiber bundles containing more than three single fibers were not performed because of difficulties in counting the number of fibers in the bundle. From these results, it is evident that the count is not very dependent on the angle of orientation nor on the number of fibers in the bundle--an advantage of the system. At least two modes of fiber destruction were noticed in the post-test microscopic examinations: 1) the fiber was broken so as to form a gap, but a significant part of the fiber segment remained, and 2) the fiber was burned out rather uniformly. The degree of burning of the tape in the vicinity of the fiber also showed differences in these two cases. It is believed that these phenomena were caused by the degree of contact of the fiber with the tape. An average value of 2.475 was obtained for the counts per fiber bridge.

C. Count Probability for Fiber Fragments of Fixed Length

1. Sample Preparation--Short Fiber Fragments. (Figures 7 and 8). A standard T300 carbon fiber tow containing 3000 single fibers was cut into small segments of prescribed length by precisely-spaced double razor blades (Reference 4). The segments were immersed in about 10 cc's of ethyl alcohol contained in a small glass bottle. The bottle was shaken thoroughly so that the fibers spread as single fibers homogeneously in the solvent. The solution was then drawn into an eyedropper and released onto 5.1 x 7.6 cm glass slides. The operator performed a

Fig. 7. Sample Preparation--Spreading Fiber Solution On the Glass Slides

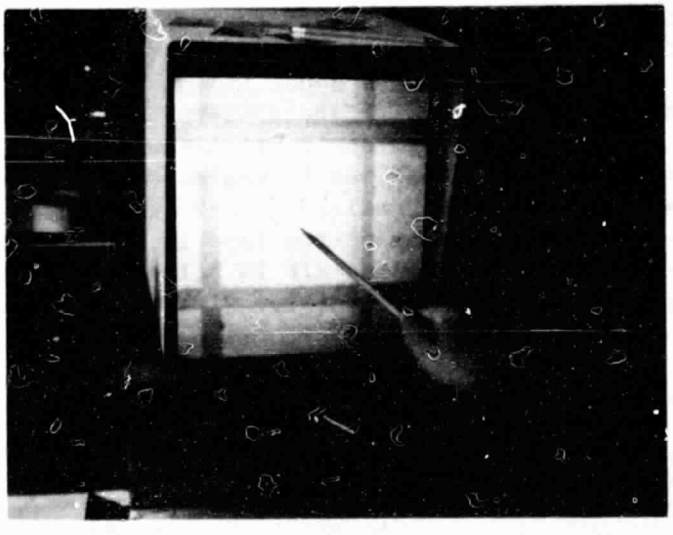

Fig. 8. Visual Counting and Inspection of the Fiber Sample

hand-motion to assure uniform spread and random fiber orientation on the slides. After the slides were dried, sticky tapes (Clear Adheer) of the same size as the glass slides were pressed onto the slides to collect the fibers.

2. Sample Preparation--Long Fiber Fragments. The technique described in C-1 was successful in preparing samples for fiber lengths up to 3.8 mm. When the fibers exceeded this length, serious agglomeration occurred. A different approach had to be adopted. An alcohol solvent containing the fibers was spread on a fine-mesh metal screen. An air-gun jet was used to purge the screen from the reverse side so that the fiber segments fell onto a large sticky tape lying at the bottom of an enclosed box. The tape was then cut to the size needed for grid counting (5.1 x 7.6 cm).

3. Visual Counting. The glass slides as prepared in C-1 and C-2 were then placed under a microfiche reader (Microcard Model 418, NCR Inc.) for visual counting. This verified the randomness of fiber orientation and the minimum number of fiber rods present in the tape. A Variac (60 VRMS) was used to control the lamp of the reader so that it would not overheat the tape, lest the tape melt and the fibers sink into the glue of the tape and be completely coated by it.

4. Spark Count Results. The sticky tapes were peeled from the glass slides and placed on the grid to be counted. These data are included in Tables B-1 through B-7, in Appendix B. In these tables, C is the total spark count per tape sample, f is the total number of fiber fragments of fixed length, C/f is the counts per fiber, $\overline{C/f}$ is the average of counts per fiber for the series of tests, and σ is the standard deviation of C/f. ΣC is the total of counts observed for the series and Σf is the total number of fibers in the series. As is evident, the total average value $\Sigma C/\Sigma f$ was very close to the average value $\overline{C/f}$ for each series. Also, for a given length of fiber, the data for different series of tests performed for samples prepared in the same way on different days were reasonably consistent.

The main features of these data are summarized in Table 2. Here $\langle C/f \rangle$ is the total average of counts/fiber of the entire data for the given fiber length and $\langle \sigma \rangle$ is the total standard deviation of C/f.

5. Comparison to the Mathematical Analysis. The data listed in Table 2, $\langle C/f \rangle$ and $\langle \sigma \rangle$, are in the form of spark counts per fiber fragment. By using the calibration factor established in V-B, above, i.e., that one fiber bridge (a segment between a pair of adjacent electrodes) corresponds to 2.475 counts, the total probability of counts for a given fiber length can be obtained. This information is plotted in Figure 9 with the theoretical data. The agreement between the experimental and mathematical results is reasonable.

6. Effect of Fiber Density. Most of the test data were gathered from sample tape with limited fiber density, i.e., the total number of fiber segments were of the order of several hundred or less per tape area of 38 cm^2. As mentioned earlier in this section, when the fiber density is high, intersections and connections between fibers themselves are inevitable, thereby affecting the accuracy of the count.

Table 2. Summary of Calibration Data

Fiber Length mm	Table Reference	Number of Tapes	Σf	ΣC	$\overline{C/f}$ x 10^{-2}	σ x 10^{-2}	⟨C/f⟩ x 10^{-2}	⟨σ⟩ x 10^{-2}
1.270		5	2565	1151	44.66	8.02		
		5	1220	472	42.42	11.26		
		6	3010	1753	58.20	7.82		
		10	3430	1313	38.90	7.84		
	B-1	12	3204	1723	52.12	17.13		
		10	2158	910	43.45	19.42	42.17	9.79
		15	3750	1586	45.11	15.43		
		15	1176	516	39.40	32.19		
		20	1000	177	16.57	7.73		
		10	3624	1418	36.86	7.10		
		9	3655	1706	44.26	13.37		
1.905		9	4409	3071	67.83	14.23		
		8	2772	3074	97.51	18.99		
		10	3660	3191	83.08	30.24		
		10	2422	2547	104.48	19.56		
	B-2	10	2199	1813	83.83	15.14	87.71	14.78
		10	1313	1204	86.31	17.83		
		10	7451	8688	113.98	22.16		
		10	666	514	86.26	50.15		
		5	158	107	66.18	21.18		
2.540	B-3	10	2674	3152	117.38	16.06	117.38	16.06
3.175	B-4	9	1284	3053	225.91	51.50	225.91	51.50
3.810		10	1025	2201	218.46	63.46		
	B-5	10	878	2038	222.80	34.97	228.92	49.07
		6	510	1293	245.50	41.05		
5.08	B-6	12	286	1153	414.18	152.97	414.18	152.97
7.62	B-7	14	681	3729	584.21	152.85	584.21	152.85

The major difficulty for such a calibration was the visual counting of the sample. A different approach was adopted. The fiber could be spread on the glass slides reasonably uniformly. As the total number of fiber segments in the alcohol was known, the number of fibers on each tape could be estimated by dividing the total number of fibers by the number of samples prepared. Experience in the preparation of low fiber density samples had shown that this assumption was reasonably valid. There was some loss of fibers during the handling and drying procedure, but this loss was less than 25%.

High fiber density samples for fiber lengths of 1.27 mm were prepared in the above manner. Test results are included in Table B-8 of Appendix B. As can be seen, the average of counts per fiber, $\overline{C/f}$ and the manner in which it varied with different test groups, was about the same as listed in Table 2. We thus conclude that the system can be used for counting high fiber density samples. The maximum

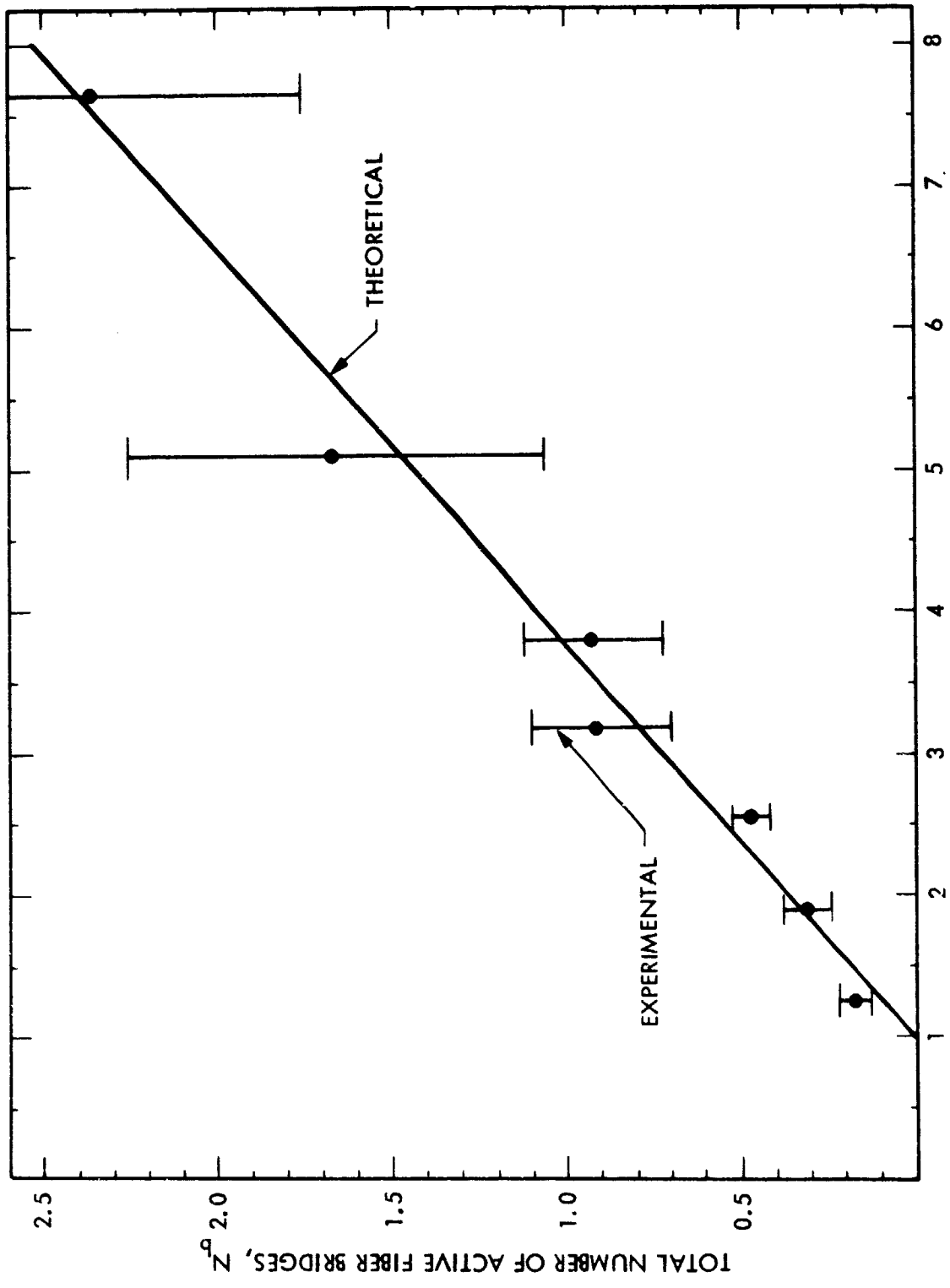

Fig. 9. Total Number of Active Fiber Bridges, N_b, as a Function of Fiber Length

fiber density tested was 7200 fibers per tape. This corresponded to a density of about 189 fibers per cm^2 (1.89×10^6 fibers/m^2 or 1.89 fibers/mm^2). It is to be noted that the tape saturation fiber density (Reference 2) would be reached at about one tenth of this value. Therefore, we conclude that the system is applicable for sticky tape sampling in the fiber density range where it has meaningful measurements for the carbon fiber exposure.

7. Accuracy Assessment. The standard deviation observed in this calibration was about 20%. Several factors might have contributed to the variation. First, the randomization of fiber orientation was controlled manually during the coating of the glass slides with the fiber solution. This procedure is certainly not perfect. Second, the thick fiber rods (strips) containing a large number of fibers could introduce more fluctuation into the spark counts, because their destruction by the sparks was more complicated and intrinsically more random.

The fluctuation in counting accuracy tends to average out by itself when a large number of tests are performed. In the practical application of large tape samples, such as vugraph-size tape, many smaller samples suitable for grid counting can be prepared, thereby establishing better statistical data. For smaller tape samples, such as the sticky cylinders, it is preferable to expose several samples to the fiber flux under the same test conditions in order to improve the accuracy of the count. The latter approach was usually used in the earlier tests of carbon fiber exposure. With the fast read-out of the H.V. grid system, simplified data reduction procedures can be achieved.

In case the tape sample does not have random fiber orientation, the following procedure is recommended for the H.V. grid test. At least two samples should be tested, one with the preferable fiber direction aligned with the grid electrodes, and the other with the direction aligned perpendicularly to the grid electrodes. An average of the two counts so obtained will provide an accurate count of the fibers.

VI. METHOD FOR TEST DATA REDUCTION

We will now describe the detailed derivation of the formulas for data reduction that were mentioned briefly in Section III.

A. Total Counts as a Function of Fiber Length

The data shown in Figure 9 shows essentially a linear relationship

$$P_b(\ell) = K\,(\ell - 1) \tag{1}$$

where $P_b(\ell)$ = The total count probability of fiber bridges* for a fiber of length ℓ
ℓ = Fiber length in mm
K = Proportionality constant
= 0.3628 mm^{-1}

Since one fiber bridge creates an average count of 2.475, we obtain the relationship:

$$P_C(\ell) = 2.475K\,(\ell - 1)$$
$$= 0.898\,(\ell - 1)\ \text{(counts)} \tag{2}$$

where $P_C(\ell)$ = The total spark count probability for a fiber of length ℓ

B. Fiber Number Distribution as a Function of Fiber Length

As previously indicated in References 1 and 2, the distribution is exponential, i.e.,

$$n(\ell) = \frac{1}{\ell_o}\, e^{-(\ell-1)/\ell_o},\ 1\ \text{mm} < \ell < \infty \tag{3}$$

where ℓ is the fiber length in millimeters. Note that

$$\int_1^\infty n(\ell)\, d\ell = 1$$

ℓ_o is a characteristic length. It is related to the mean fiber length $\bar{\ell}$ by the following relation.

$$\bar{\ell} = \int_1^\infty \ell\, n\, d\ell$$

$$= \ell_o + 1$$

---

* including partial fiber bridges which allow the spark to occur, i.e., air gap less than 0.19 mm.

An approximate typical value of ℓ_o is 2.2 mm (Reference 2). This representation is not correct when fibers less than 1 mm are considered. In NASA's "Carbon Fiber Risk Analysis" work, the number of fibers in this short fiber length regime was found to be small and was not included in the analysis. The H.V. Grid Carbon Fiber Sticky Tape Analyzer was designed to measure only fibers longer than 1 mm.

C. The Physical Meaning of the Total Spark Count

By using Equations (2) and (3), the total counts, C, can be calculated as follows:

$$C = \int_1^\infty NP_C(\ell)n(\ell)d\ell$$

$$= \int_1^\infty Nk(\ell - 1)\frac{1}{\ell_o} e^{-(\ell-1)/\ell_o} d\ell \qquad (4)$$

$$= Nk\ell_o$$

therefore,

$$N = \text{Total number of fibers on the tape}$$

$$= \frac{C}{k\ell_o} \qquad (5)$$

Note that

$N\,n(\ell)$ = Number of fibers with length ℓ on the tape

The total length of fiber, L, on the tape can be calculated as

$$L = \int_1^\infty \ell Nn(\ell)\, d\ell$$

$$= N\bar{\ell}$$

$$= N(\ell_o + 1)$$

$$= \frac{C}{k}\left(1 + \frac{1}{\ell_o}\right) \qquad (6)$$

By assuming a prio i knowledge of the fiber length distribution we can obtain crucial information regarding the total number of fibers and total fiber mass (length) collected on the tape.

VII. CONCLUDING REMARKS

In this project we have successfully accomplished the following tasks:

1) We have achieved a statistical understanding of spark counts initiated by carbon fibers collected on a sticky tape in contact with a H.V. grid system.

2) We have obtained sufficient data to establish a calibration factor for the counting of carbon fibers on sticky tape samples.

3) We have developed prototype hardware and demonstrated its satisfactory performance in laboratory tests, namely its

   a) fast counting capability

   b) counting accuracy

   c) fiber density limitations

   d) system durability

The current system is believed to be suitable for the majority of sticky tape samples containing carbon fibers, and can be used as a standard test for these types of sticky tape. Under the current design, the system is not affected by the presence of soot on the tape. The system could be applied to counting carbon fibers collected on micropore filters; however, a calibration procedure similar to that used in this work should be performed to assure that the physical differences between a sticky tape and a micropore filter do not change the calibration.

APPENDIX A

MATHEMATICAL MODELING

The problem is to determine the mathematical probability of a conductive carbon fiber producing a number of sparks when brought into contact with an H.V.-biased grid. The grid is composed of parallel copper plates 0.51 mm wide placed such that a gap of 1.19 mm exists between two adjacent pairs of electrode surfaces. Previous experiments have shown that a spark will result if a fiber bridges more than 84% of the gap. With this information, it is possible to determine the conditions necessary for spark production for a fiber of a given fixed length.

The following discussion is based on a similar problem (Buffon's problem) solved by Kendall and Moran (Reference 5). For the benefit of cross referencing, the mathematical notations used in the book are adopted here for the discussion.

Consider a fiber of length L in contact with the grid as is shown in Figure A-1. In order for two intersections (one spark) to occur, the following condition must be satisfied.

$$L\sin\theta \geq BD \tag{A-1}$$

where B is the fraction of gap width (84%) necessary for a spark. Similarly, for three intersections (two sparks), one obtains

$$L\sin\theta \geq 2\,BD + W \tag{A-2}$$

For four intersections (three sparks), the condition is

$$L\sin\theta \geq 2\,BD + W + (D + W) \tag{A-3}$$

For K intersections (K - 1 sparks), the condition can be generalized as follows:

$$L\sin\theta \geq 2\,BD + W + (K - 3)\,(D + W)\ , \quad K \geq 3 \tag{A-4}$$

Furthermore, given a fiber of length L such that

$$L = 2\,BD + W + (n - 2)\,(D + W) + \ell\ , \quad n \geq 2 \tag{A-5}$$

where n is an integer and $\ell < BD$, the maximum number of intersections is n + 1. The probability for n + 1 intersections is given by

$$P_{n+1} = \frac{2}{\pi D_1}\int_{\alpha_n}^{\pi/2} [L\sin\theta - 2\,BD - W - (n - 2)\,D_1]\,d\theta \tag{A-6}$$

where $L\sin\alpha_n = 2\,BD + W + (n - 2)\,(D + W)$, $D_1 = W + D$, $n \geq 2$

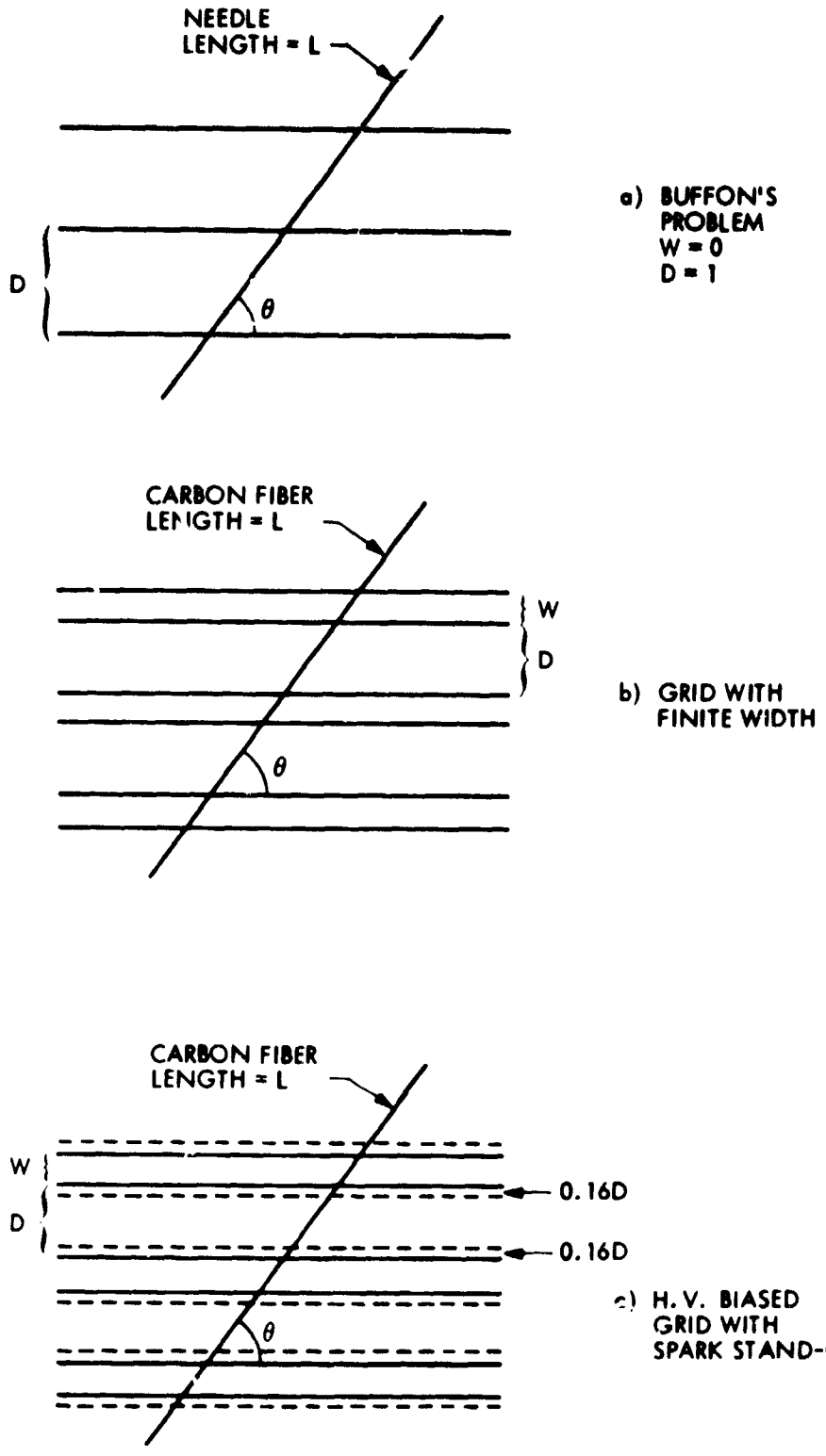

Fig. A-1. Schematic Representation of the Mathematical Model

Evaluating the integral gives

$$P_{n+1} = \frac{2L}{\pi D_1} \cos\alpha_n + \frac{2}{\pi D_1} [2\ BD + W + (n - 2)D_1]\ (\alpha_n - \pi/2) \qquad \text{(A-7)}$$

The probability of K intersections, for $K < n + 1$, is

$$P_K = \frac{2}{\pi D_1} \int_{\alpha_{K-1}}^{\alpha_K} [L\sin\theta - 2\ BD - W - (K - 3)D_1]d\theta \qquad \text{(A-8)}$$

$$+ \frac{2}{\pi D_1} \int_{\alpha_K}^{\alpha_{K+1}} [2\ BD + W + (K - 1)D_1 - L\sin\theta]d\theta$$

$$= \frac{2}{\pi D_1} \Big\{ [2\ BD + W + (K - 3)D_1]\alpha_{K-1}$$

$$- 2[2\ BD + W + (K - 2)D_1]\alpha_K$$

$$+ [2\ BD + W + (K - 1)D_1]\alpha_{K+1} \Big\} \qquad \text{(A-9)}$$

$$+ \frac{2L}{\pi D_1} [\cos\alpha_{K-1} - 2\cos\alpha_K + \cos\alpha_{K+1}]$$

where $L\sin\alpha_K = 2\ BD + W + (K - 2)D_1$, unless $K = n$; then $\alpha_K = \pi/2$.

There is also a special case when two intersections occur. In this situation the probability equations must be modified. If only two intersections can occur, then

$$P_2 = \frac{2}{\pi D_1} \int_{\alpha_1}^{\pi/2} [L\sin\theta + D - 2\ BD]d\theta \qquad \text{(A-10)}$$

where $L\sin\alpha_1 = BD$

If more than two intersections are possible

$$P_2 = \frac{2}{\pi D_1} \int_{\alpha_1}^{\alpha_2} [L\sin\theta + D - 2\ BD]d\theta \qquad \text{(A-11)}$$

$$+ \frac{2}{\pi D_1} \int_{\alpha_2}^{\alpha_3} [2\ BD + W + D_1 - L\sin\theta]d\theta$$

The value of α_1 is defined following equation A-10, and the values of α_2 and α_3 are defined following equation A-9.

With the aid of equations A-7, A-9, A-10, and A-11, it is possible to determine the number of shorts (active fiber bridges which can produce sparks across a pair of adjacent electrodes) occurring as a function of fiber length by multiplying the probability of a given number of intersections by the number of shorts resulting from the intersections. Thus, if N_b is the number of shorts,

$$N_b = \sum_{i=2}^{n+1} P_i \, (i - 1) \qquad \text{(A-12)}$$

when n + 1 is the maximum number of intersections possible. Because of the number and complexity of the equations used, a computer program was developed to perform the calculations. A listing of the program is shown in Table A-1. The program consists of selecting a fiber length and determining the probability of two intersections occurring, then three, four, etc., until the probability for the maximum number of intersections has been found. The probabilities are multiplied by the number of shorts resulting from the intersections, and this product summed as shown in Equation A-12. A range of fiber lengths are run and the results are shown in Table A-2 and graphed in Figure 9 along with the experimentally determined results. The agreement between them is good in the entire fiber length region under study.

Table A-1. A Computer Program for the Mathematical Modeling Study

```
10 DIM A[5]
20 D1=1.19+0.508
30 D2=0.84*1.19
40 W=0.508
50 D=1.19
60 DEF FNA(X)=ATN(X/SQR(1-X*X+1E-99))
70 DEF FNC(K)=FNA(((2*D2+W+(K-2)*D1)/L))
80 FOR L=1 TO 8 STEP 0.25
90 P=0
100 FOR K=2 TO 8 STEP 1
110 IF K>2 THEN 410
120 IF L <= D2+(K-1)*D1 THEN 280
130 A1=FNA(D2/L)
140 A2=FNC(K)
150 IF L<D2+K*D1 THEN 180
160 A3=FNC(K+1)
170 GOTO 190
180 A3=PI/2
190 P1=(2*D2-D)*A1
200 P2=(4*D2-D+W+D1)*A2
210 P3=(  *D2+W+D1)*A3
220 P4=COS(A1)-2*COS(A2)+COS(A3)
230 P0=(2/(PI*D1))*(P1-P2+P3+L*P4)
240 PRINT L,K,P0
250 P0=P0*(K-1)
260 P=P+P0
270 NEXT K
280 IF K>2 THEN 320
290 A1=FNA(D2/L)
300 P0=(2/(PI*D1))*(L*COS(A1)+(2*D2-D)*(A1-PI/2))
310 GOTO 340
320 A1=FNC(K-1)
330 P0=(2/(PI*D1))*(L*COS(A1)+((K-3)*D1+W+2*D2)*(A1-PI/2))
340 PRINT L,K,P0
350 P0=P0*(K-1)
360 P=P+P0
370 PRINT L;K,"P TOTAL";P
380 PRINT
390 NEXT L
400 GOTO 580
410 IF L <= 2*D2+W+(K-2)*D1 THEN 280
420 A1=FNC(K-1)
430 A2=FNC(K)
440 IF L<2*D2+W+(K-1)*D1 THEN 470
450 A3=FNC(K+1)
460 GOTO 480
470 A3=PI/2
480 P1=((K-1)*D1+D2*2+W)*A3
490 P2=2*((K-2)*D1+2*D2+W)*A2
500 P3=((K-3)*D1+2*D2+W)*A1
510 P4=COS(A3)-2*COS(A2)+COS(A1)
520 P0=(2/PI)*(P1-P2+P3+L*P4)
530 P0=P0/D1
540 PRINT L,K,P0
550 P0=P0*(K-1)
560 P=P+P0
570 GOTO 270
580 END
```

Table A-2. Results of Mathematical Analysis

Fiber Length L(mm)	P_i Probability of i Intersections 2	3	4	5	6	Total Number of Shorts N_b
1.00	2.2×10^{-3}					2.2×10^{-3}
1.25	0.086					0.086
1.50	0.164					0.1 ,
1.75	0.246					0.246
2.00	0.332					0.332
2.25	0.419					0.419
2.50	0.507					0.507
2.75	0.545	0.025				0.597
3.00	0.544	0.071				0.687
3.25	0.524	0.127				0.778
3.50	0.490	0.190				0.869
3.75	0.446	0.257				0.960
4.00	0.395	0.329				1.052
4.25	0.338	0.399	0.002			1.143
4.50	0.303	0.426	0.027			1.236
4.75	0.277	0.427	0.066			1.329
5.00	0.256	0.413	0.113			1.421
5.25	0.239	0.388	0.166			1.514
5.50	0.224	0.354	0.224			1.607
5.75	0.211	0.314	0.287			1.699
6.00	0.200	0.272	0.344	0.004		1.792
6.25	0.190	0.246	0.363	0.029		1.885
6.50	0.181	0.226	0.363	0.064		1.978
6.75	0.173	0.211	0.350	0.107		2.071
7.00	0.166	0.198	0.328	0.155		2.164
7.25	0.159	0.186	0.299	0.207		2.258
7.50	0.153	0.177	0.264	0.263		2.351
7.75	0.147	0.168	0.230	0.308	0.007	2.444
8.00	0.142	0.161	0.210	0.322	0.032	2.537

APPENDIX B

DETAILED CALIBRATION TEST DATA

Table B-1. Test Data for 1.27 mm Fiber

Tape No.	f	C	C/f $\times 10^{-2}$
1	528	206	39.0
2	570	333	58.4
3	530	185	34.9
4	477	224	46.9
5	460	203	44.1
	$\Sigma f = 2565$	$\Sigma C = 1151$	$\overline{C/f} = 44.66$
	$\Sigma C/\Sigma f = 44.87$		$\sigma = 8.02$
1	117	72	61.5
2	193	88	45.5
3	255	109	42.7
4	364	106	29.1
5	291	97	33.3
	$\Sigma f = 1220$	$\Sigma C = 472$	$\overline{C/f} = 42.42$
	$\Sigma C/\Sigma f = 38.69$		$\sigma = 11.266$

Table B-1. Test Data for 1.27 mm Fiber (Continuation 1)

Tape No.	f	C	C/f $\times 10^{-2}$
1	532	256	48.1
2	495	356	71.9
3	552	352	63.7
4	454	238	52.4
5	432	253	58.5
6	545	298	54.6
	$\Sigma f = 3010$	$\Sigma C = 1753$	$\overline{C/f} = 58.20$
	$\Sigma C/\Sigma f = 58.23$		$\sigma = 7.82$
1	480	198	41.2
2	428	165	38.5
3	397	101	25.4
4	356	113	31.7
5	391	118	30.1
6	266	107	40.2
7	298	132	44.2
8	230	101	43.9
9	295	161	54.5
10	297	117	39.3
	$\Sigma f = 3438$	$\Sigma C = 1313$	$\overline{C/f} = 38.9$
	$\Sigma C/\Sigma f = 38.19$		$\sigma = 7.84$

Table B-1. Test data for 1.27 mm Fiber (Continuation 2)

Tape No.	f	C	C/f $\times 10^{-2}$
1	217	73	33.6
2	238	70	29.4
3	307	150	48.8
4	396	352	88.8
5	269	93	34.5
6	312	114	36.5
7	210	146	69.5
8	283	190	67.1
9	206	98	47.5
10	229	117	51.0
11	277	184	66.4
12	260	136	52.3
	$\Sigma f = 3204$	$\Sigma C = 1723$	$\overline{C/f} = 52.12$
		$\Sigma C/\Sigma f = 53.77$	$\sigma = 17.13$
1	157	36	22.9
2	175	92	52.5
3	252	130	51.5
4	280	75	26.7
5	228	63	27.6
6	274	150	54.7
7	148	135	91.2
8	197	79	40.1
9	217	85	39.1
10	230	65	28.2
	$\Sigma f = 2158$	$\Sigma C = 910$	$\overline{C/f} = 43.45$
		$\Sigma C/\Sigma f = 42.17$	$\sigma = 19.42$

Table B-1. Test Data for 1.27 mm Fiber (Continuation 3)

Tape No.	f	C	C/f $\times 10^{-2}$
1	328	90	27.4
2	298	131	44.0
3	368	151	41.0
4	154	101	66.0
5	279	110	39.4
6	328	82	25.0
7	275	97	35.3
8	225	105	47.0
9	210	184	88.0
10	186	73	39.2
11	97	57	59.0
12	187	92	49.2
13	231	102	44.2
14	236	76	33.2
15	348	135	38.8
	$\Sigma f = 3750$	$\Sigma C = 1586$	$\overline{C/f} = 45.11$
		$\Sigma C/\Sigma f = 42.29$	$\sigma = 15.43$
1	69	16	23.0
2	98	109	111.0
3	64	9	14.0
4	68	24	35.2
5	80	16	20.0
6	40	8	20.0
7	96	23	23.9
8	73	12	16.4
9	74	23	31.0
10	84	81	96.4
11	111	21	18.9
12	69	20	28.9
13	73	38	52.0
14	120	112	93.0
15	57	4	7.0
	$\Sigma f = 1176$	$\Sigma C = 516$	$\overline{C/f} = 39.40$
		$\Sigma C/\Sigma f = 43.87$	$\sigma = 32.19$

Table B-1. Test Data for 1.27 mm Fiber (Continuation 4)

Tape No.	f	C	C/f x 10^{-2}
1	31	9	29.0
2	63	17	26.9
3	46	11	23.9
4	84	11	13.1
5	51	7	13.7
6	58	4	6.9
7	56	6	10.7
8	56	11	19.6
9	43	2	4.6
10	37	7	18.9
11	74	15	20.3
12	45	13	28.9
13	79	10	12.7
14	43	7	16.3
15	67	17	25.4
16	51	2	3.9
17	60	12	20.0
18	28	4	14.3
19	70	10	14.3
20	25	2	8.0
	$\Sigma f = 1000$	$\Sigma C = 177$	$\overline{C/f} = 16.57$
		$\Sigma C/\Sigma f = 17.7$	$\sigma = 7.73$
1	326	121	37.1
2	190	53	27.8
3	269	79	29.3
4	419	140	33.4
5	269	79	29.3
6	427	206	42.2
7	387	174	44.9
8	492	231	46.9
9	468	214	45.7
10	377	121	32.0
	$\Sigma f = 3624$	$\Sigma C = 1418$	$\overline{C/f} = 36.86$
		$\Sigma C/\Sigma f = 39.13$	$\sigma = 7.10$

Table B-1. Test Data for 1.27 mm Fiber (Continuation 5)

Tape No.	f	C	C/f $\times 10^{-2}$
1	630	423	67.1
2	310	65	21.0
3	367	212	57.7
4	361	152	42.1
5	544	247	45.4
6	294	125	42.5
7	224	68	30.4
8	331	198	37.3
9	394	216	54.8
	$\Sigma f = 3655$	$\Sigma C = 1706$	$C/f = 44.26$
		$\Sigma C/\Sigma f = 46.67$	$\sigma = 13.37$

Table B-2. Test Data for 1.905 cm Fiber

Tape No.	f	C	C/f $\times 10^{-2}$
1	507	308	60.7
2	529	314	59.3
3	617	424	68.7
4	583	440	75.4
5	402	215	53.4
6	347	170	48.9
7	587	564	96.0
8	339	217	64.0
9	498	419	84.1
	$\Sigma f = 4409$	$\Sigma C = 3071$	$\overline{C/f} = 67.83$
		$\Sigma C/\Sigma f = 69.65$	$\sigma = 14.22$
1	370	265	71.6
2	447	443	99.1
3	368	459	124.7
4	368	250	67.9
5	376	327	86.9
6	360	408	113.3
7	427	467	109.3
8	424	455	107.3
	$\Sigma f = 2772$	$\Sigma C = 3074$	$\overline{C/f} = 97.51$
		$\Sigma C/\Sigma f = 110.89$	$\sigma = 18.99$

Table B-2. Test Data for 1.905 mm Fiber (Continuation 1)

Tape No.	f	C	C/f $\times 10^{-2}$
1	401	393	98.0
2	248	157	63.3
3	328	193	58.8
4	365	435	119.1
5	342	421	123.0
6	277	180	38.8
7	368	309	83.9
8	495	596	120.4
9	374	313	83.6
10	462	194	41.9
	$\Sigma f = 3660$	$\Sigma C = 3191$	$\overline{C/f} = 83.08$
		$\Sigma C/\Sigma f = 87.18$	$\sigma = 30.24$
1	205	206	100.4
2	258	256	99.2
3	315	364	115.5
4	222	206	92.7
5	295	420	142.3
6	239	228	95.3
7	251	250	99.6
8	173	167	96.5
9	268	190	70.8
10	196	260	132.5
	$\Sigma f = 2422$	$\Sigma C = 2547$	$\overline{C/f} = 104.48$
		$\Sigma C/\Sigma f = 105.16$	$\sigma = 19.50$

Table B-2. Test Data for 1.905 mm Fiber (Continuation 2)

Tape No.	f	C	C/f x 10^{-2}
1	292	231	79.3
2	204	204	100.0
3	282	164	58.1
4	176	120	68.1
5	205	227	110.0
6	142	137	96.4
8	219	194	88.5
8	249	191	76.7
9	226	162	71.6
10	204	183	89.7
	$\Sigma f = 2199$	$\Sigma C = 1813$	$\overline{C/f} = 83.83$
		$\Sigma C/\Sigma f = 82.44$	$\sigma = 15.14$
1	98	85	86.7
2	81	59	72.8
3	110	98	89.0
4	140	115	82.1
5	106	86	81.1
6	129	106	82.1
7	147	101	68.7
8	257	354	137.0
9	110	92	83.6
10	135	108	80.0
	$\Sigma f = 1313$	$\Sigma C = 1204$	$\overline{C/f} = 86.31$
		$\Sigma C/\Sigma f = 91.69$	$\sigma = 17.83$

Table B-2. Test Data for 1.905 mm Fiber (Continuation 3)

Tape No.	f	C	C/f $\times 10^{-2}$
1	876	1056	120.5
2	763	663	86.2
3	828	1159	139.9
4	914	1385	151.5
5	670	734	109.5
6	657	843	128.3
7	513	402	78.3
8	718	721	100.4
9	670	668	99.7
10	842	1057	125.5
	$\Sigma f = 7451$	$\Sigma C = 8688$	$\overline{C/f} = 113.98$
		$\Sigma C/\Sigma f = 116.60$	$\sigma = 22.16$
1	51	74	145.0
2	69	33	47.8
3	65	24	36.9
4	74	35	47.2
5	83	24	28.9
6	100	58	58.0
7	75	87	116.0
8	41	68	165.8
9	61	39	63.9
10	47	72	153.1
	$\Sigma f = 666$	$\Sigma C = 514$	$\overline{C/f} = 96.26$
		$\Sigma C/\Sigma f = 77.17$	$\sigma = 50.15$

Table B-2. Test Data for 1.905 mm Fiber (Continuation 4)

Tape No.	f	C	C/f x 10^{-2}
1	22	13	59.0
2	48	42	87.5
3	25	24	96.0
4	33	16	48.4
5	30	12	40.0
	$\Sigma f = 158$	$\Sigma C = 107$	$\overline{C/f} = 66.18$
		$\Sigma C/\Sigma f = 67.72$	$\sigma = 21.89$

Table B-3. Test Data for 2.54 mm Fiber

Tape No.	f	C	C/f x 10^{-2}
1	233	317	136.0
2	282	319	113.1
3	242	264	109.0
4	191	217	113.6
5	317	499	157.4
6	271	320	118.0
7	308	340	110.3
8	279	310	111.1
9	242	253	104.2
10	309	313	101.2
	$\Sigma f = 2674$	$\Sigma C = 3152$	$\overline{C/f} = 117.38$
		$\Sigma C/\Sigma f = 117.87$	$\sigma = 16.06$

Table B-4. Test Data for 3.175 mm Fiber

Tape No.	f	C	C/f x10^{-2}
1	243	834	343.2
2	97	153	157.7
3	140	380	271.4
4	125	306	244.8
5	157	295	187.8
6	156	340	217.9
7	111	224	201.8
8	148	302	204.0
9	107	219	204.6
	$\Sigma f = 1284$	$\Sigma C = 3053$	$\overline{C/f} = 225.91$
		$\Sigma C/\Sigma f = 237.77$	$\sigma = 51.50$

Table B-5. Test Data for 3.81 mm Fiber

Tape No.	f	C	C/f x 10^{-2}
1	100	181	181.0
2	96	173	180.2
3	158	254	160.7
4	87	107	122.9
5	92	175	190.2
6	96	251	261.4
7	106	212	200.0
8	112	296	264.2
9	84	291	346.4
10	94	261	277.6
	$\Sigma f = 1025$	$\Sigma C = 2201$	$\overline{C/f} = 218.46$
		$\Sigma C/\Sigma f = 214.73$	$\sigma = 63.46$
1	107	228	213.0
2	140	424	302.8
3	41	84	204.8
4	133	368	276.6
5	44	91	206.8
6	68	142	208.8
7	101	219	216.8
8	65	140	215.3
9	108	204	188.8
10	71	138	194.3
	$\Sigma f = 878$	$\Sigma C = 2038$	$\overline{C/f} = 222.80$
		$\Sigma C/\Sigma f = 232.12$	$\sigma = 34.97$

Table B-5. Test Data for 3.81 mm Fiber (Continuation 1)

Tape No.	f	C	C/f x 10^{-2}
1	90	257	285.5
2	121	361	298.3
3	41	87	212.1
4	111	256	230.6
5	80	202	252.5
6	67	130	194.0
	Σf = 510	ΣC = 1293	$\overline{C/f}$ = 245.50
		$\Sigma C/\Sigma f$ = 253.5	σ = 41.05

Table B-6. Data for 5.08 mm Fiber

Tape No.	f	C	C/f x 10^{-2}
1	16	42	262.5
2	21	85	404.7
3	26	82	315.3
4	35	194	554.2
5	12	85	708.3
6	22	80	362.6
7	37	95	256.7
8	21	62	295.2
9	38	176	463.1
10	14	39	278.5
11	29	109	375.8
12	15	104	693.3
	Σf = 286	ΣC = 1153	$\overline{C/f}$ = 414.18
		$\Sigma C/\Sigma f$ = 403.14	σ = 152.97

Table B-7. Test Data for 7.65 mm Fiber

Tape No.	f	C	C/f $\times 10^{-2}$
1	34	150	441
2	61	316	519
3	29	173	597
4	46	243	528
5	23	209	909
6	39	220	564
7	48	304	633
8	78	336	431
9	53	268	506
10	64	300	469
11	27	258	956
12	67	334	499
13	32	189	591
14	80	429	536
	$\Sigma f = 681$	$\Sigma C = 3729$	$\overline{C/f} = 584.21$
		$\Sigma C/\Sigma f = 547.57$	$\sigma = 152.85$

Table B-8. High Fiber Density Tape Test Data for 1.27 mm Fiber

Group	No. of Tapes	$\bar{f}$	C	$\overline{C/f}$ x 10^{-2}	σ x 10^{-2}
1	10	6000	1564	25.9	11.3
2	10	4800	1970	41.0	6.4
3	10	2400	823	34.2	9.0
4	5	4800	3788	78.8	20.1
5	5	4800	2747	57.2	16.7
6	5	2400	1539	64.1	5.1
7	5	2400	1102	45.9	7.7
8	5	4800	2269	47.2	10.5
9	5	2400	718	29.9	8.9
10	5	2400	1492	62.1	11.9
11	5	1200	682	56.8	10.7
12	5	1200	334	27.9	9.5
13	5	7200	6890	95.6	9.4
14	5	1800	657	36.5	6.7
15	5	1800	567	31.5	11.8
16	10	600	143	23.9	6.8
17	20	750	306	40.7	11.5
18	5	3600	1734	48.1	8.4
19	10	750	131	17.4	4.8
20	5	6000	2176	36.2	6.4
			Average	45.04	9.6

* $\bar{f} = \frac{\text{Total No. of Fibers}}{\text{No. of Tapes}}$

APPENDIX C

ADDITIONAL INFORMATION FOR THE H.V. SPARK CARBON FIBER REAL-TIME DETECTION SYSTEM

The carbon fiber sample handling technique developed in the work of this report was successfully used to perform a live fiber counting accuracy test for the H.V. spark carbon fiber real-time detection system reported in Reference 4.

Two 1.27 mm long segments of carbon fiber were cut from a standard carbon fiber tow which contained 3000 individual single fibers. The sample was immersed in 10 cc of ethyl alcohol and shaken thoroughly as described in Section V. The solution, which contained separated fibers, was allowed to spread on a 200 mesh sieve to dry out the alcohol. The sieve was then placed under the glass funnel of the JPL chimney test (Section X-A, Reference 4, with the fiber side facing a No. 1 (1 mm) H.V. grid - windbox assembly sealed at the top of the chimney. A low pressure air gun was used to purge the sieve so that the fibers were released and flowed into the H.V. grid.

The total of counts so detected was in agreement with the total number of fibers tested. The agreement was within +3% for several tests performed.

REFERENCES

1. "Carbon Fiber Risk Analysis," NASA Conference Publication 2074, an industry/government briefing held at Langley Research Center, Hampton, Virginia, October 31 - November 1, 1978.

2. "Carbon Fiber Hazard," NASA Conference Publication No. 2119, an industry/government briefing held at Langley Research Center, Hampton, Virginia, December 4-5, 1979.

3. T. C. Babinsky and K. A. Musselman, "Burn/Blast Tests of Aircraft Structure Elements," NSWC/DL, TR-3897, December 1978.

4. L. C. Yang, "High Voltage Spark Carbon Fiber Detection System," JPL Publication 80-30, April 15, 1980.

5. M. G. Kendall and P. A. P. Moran, Geometrical Probability, Hafner Publishing Co., New York (1963).